Letters

Mismatches in thermal and nutrient physiology predict competitive outcomes among phytoplankton

Short running title: Physiological mismatches predict competition

Elvire Bestion[1*], Bernardo Garcia-Carreras[2], Charlotte-Elisa Schaum[1], Samraat Pawar[2], Gabriel Yvon-Durocher[1*]

[1]Environment and Sustainability Institute, University of Exeter, Penryn, Cornwall TR10 9EZ, UK

[2] Department of Life Sciences, Imperial College London, Silwood Park Campus, Ascot, Berkshire, SL5 7PY, UK

e.bestion@exeter.ac.uk, bernardo.garcia-carreras08@imperial.ac.uk, C.L.Schaum@exeter.ac.uk, s.pawar@imperial.ac.uk, g.yvon-durocher@exeter.ac.uk

*** Corresponding authors:**

Elvire Bestion

Environment and Sustainability Institute, University of Exeter, Penryn, Cornwall TR10 9EZ, UK Add phone + fax Email: e.bestion@exeter.ac.uk

Gabriel Yvon-Durocher

Environment and Sustainability Institute, University of Exeter, Penryn, Cornwall TR10 9EZ, UK Add phone + fax Email: g.yvon-durocher@exeter.ac.uk

Statement of authorship: GYD and SP conceived the study. EB and GYD designed the experiment, EB performed the experiment, SP and BGC wrote the theory. EB and BGC analysed the data, EB wrote the first draft and all authors contributed to writing.

Data accessibility: data will be available on dryad upon publication

Keywords: nutrients, phosphate, global changes, climate change, interspecific competition, trait-based ecology

Number of words in the abstract:

Number of words in the main text:

Number of references:

Number of figures, tables and text boxes:

Abstract

Current climate change affects species through both direct effects of temperature on species physiology and indirect effects of temperature on species interactions. To better predict the consequences of future climate change, it is thus crucial to understand how increased temperatures affect species interactions. Recent theoretical studies have demonstrated the potential for mismatches between prey and predators' thermal physiology to alter consumer-resource dynamics. However fewer resources have been devoted to explaining interspecific competition, and, to our knowledge, no large experimental study has tackled this issue to build a bridge between theory and experiments. Here we investigated how mismatches in competing species' thermal and nutrient physiology affected the outcome of the competition in phytoplankton. We developed a theoretical model based on the Monod model of nutrient physiology to investigate competition between species, and tested the predictions of this model against a large scale competition experiment of six species of freshwater phytoplankton at two temperatures and two nutrient conditions. We show that competitive outcomes are driven by mismatches in species maximum growth rates $\mu_{\max}$ and half-saturation constant K_S. Further, reversals in competitive outcomes with temperature were linked to temperature-driven reversals in nutrient physiology traits $\mu_{\max}$ and K_S.

Introduction

Climate change is predicted to be a major cause of species extinctions over the next century (Field *et al.* 2014), and a considerable threat to biodiversity (Thomas *et al.* 2004; Bellard *et al.* 2012). Susceptibility to climate change will depend on species' environmental tolerances (Pacifici *et al.* 2015), with those occupying narrower thermal niches expected to be more vulnerable to climate warming (Magozzi & Calosi 2015). However, recent studies have highlighted that species interactions may play a greater role in mediating the impacts of climate change on populations than physiological tolerance limits (Dunn *et al.* 2009; Bellard *et al.* 2012; Cahill *et al.* 2013; Field *et al.* 2014). Indeed the key drivers of global change (warming, CO_2 and nutrient enrichment) are known to affect various types of species interactions, including competition (Tylianakis *et al.* 2008). To better predict the consequences of future climate change, it is therefore crucial to understand how increased temperatures affect species interactions (Bestion & Cote 2017).

Metabolism sets the pace of life (Brown *et al.* 2004) and dictates a host of life-history traits and attributes that determine fitness, including population growth rate (Savage *et al.* 2004), abundance, mortality and interspecific interactions (Dell *et al.* 2011). Species vary widely in the way in which their metabolism and associated traits respond to temperature (Kingsolver 2009; Dell *et al.* 2011), and these differences in thermal physiology can greatly impact species interactions (Reuman *et al.* 2014; Dell *et al.* 2014). Mismatches can arise when species' metabolic traits differ in their magnitude (the elevated of thermal performance curve), sensitivity to temperature (the slope of their temperature-performance relationship) and/or thermal optima (the temperature at which the performance is maximised) (Kordas *et al.* 2011). Recent theory suggests that mismatches in the thermal responses of body velocity between interacting species can play a key role in shaping the effects of temperature on consumer-resource dynamics (Dell *et al.* 2014). Mismatches in the temperature-dependence of metabolic rate, nutrient supply rate, consumer consumption efficiency and mortality rates all have the potential to affect biomass fluxes between consumers and resources, and in turn, the stability of food webs (Gilbert *et al.* 2014). In plant-herbivore interactions, higher temperature-dependence of heterotroph respiration compared to photosynthesis has been predicted to increase the strength of top down control in aquatic ecosystems (O'Connor *et al.* 2011). However, while there have major advances in ecological theory, linking the effects of temperature to metabolism and species interactions (O'Connor *et al.* 2011; Dell *et al.* 2014; Gilbert *et al.* 2014; Amarasekare 2015; Uszko *et al.* 2017), there have been very few empirical tests of this theory, and to our knowledge, no large scale experimental study has confronted recent theoretical developments to test how mismatches in thermal physiology drive the outcome of species interactions.

In aquatic ecosystems, temperature and nutrients are the two main drivers of phytoplankton productivity (Litchman *et al.* 2010). The effects of temperature on phytoplankton growth typically follow a characteristic left-skewed unimodal function, where rates increase exponentially to an optimum followed by a steeper exponential decline. Phytoplankton exhibit substantial variation among species and functional groups in these thermal response curves (Thomas *et al.* 2016) and interspecific variation in thermal tolerance can be an important driver of community dynamics and seasonal succession in phytoplankton communities (Grover & Chrzanowski 2006). Nutrient availability also has a major impact on phytoplankton growth, with rates typically increasing as a saturating, hyperbolic function of increasing nutrients, characterised by the Monod curve (Monod 1949). Interspecific variation in the functional traits that shape nutrient uptake and growth (e.g. the half saturation constant

and the maximum growth rate) are widely recognised to be key drivers of competition (Tilman 1981), community assembly (Bulgakov & Levich 1999) and ultimately the productivity of phytoplankton communities (Behrenfeld *et al.* 2005). The non-linear effects of temperature and nutrients also interact multiplicatively. For example, temperature can influence both the half-saturation constant and the maximum growth rate (Aksnes & Egge 1991; Sterner & Grover 1998; Carter & Lathwell 1967; Mechling & Kilham 1982; Senft *et al.* 1981) and vice-versa, recent work has shown that the optimum temperature for growth increases as a saturating function of nutrient availability (Thomas *et al.* 2017). Thus changes in environmental conditions can potentially amplify mismatches between competitors' functional traits, and this could affect species competition and community assembly (Litchman *et al.* 2010; Kordas *et al.* 2011). Given that both temperature and nutrient balance are predicted to shift with global changes (IPCC 2013; Behrenfeld *et al.* 2006; Ye *et al.* 2011), understanding the potential for such climate-driven mismatches is made all the more urgent.

Here we investigate how mismatches between species thermal and nutrient traits affect competition in phytoplankton. We do so by modelling species growth rate as a function of nutrient physiology through a Monod equation (Monod 1949). Species nutrient physiology is defined by the two parameters of the model, the maximum growth rate (maximum growth rate achieved in nutrient replete conditions) and the half-saturation constant (concentration of limiting nutrient at which the growth is half of the maximum growth rate), which can themselves vary with temperature. We study how mismatches in these traits can predict competitive outcomes. We then test our model's predictions against empirical data on 6 species of freshwater phytoplankton in a large-scale experiment with all pairwise combinations of the six species at two temperature and nutrient levels.

Theory

We used the Monod equation to characterize the effects of nutrient concentration on phytoplankton growth rate. The dynamics of a single species limited by a single resource can be described as

$$\frac{1}{N}\frac{dN}{dt} = \mu = \frac{\mu_{max} S}{K_S + S} \quad (1)$$

$$\frac{dS}{dt} = -\alpha N \frac{\mu_{max} S}{K_S + S} \quad (2)$$

Where N is the phytoplankton cell density (cells·mL^{-1}), μ is the realised growth rate (d^{-1}) of the species, μ_{max} is the maximum growth rate in nutrient saturated conditions (d^{-1}), which reflects a species' performance under nutrient saturated conditions, K_S is the half-saturation constant (µmol·L^{-1}) which is a measure of performance at low nutrient concentrations, , S is the nutrient concentration (µmol·L^{-1}) and α is the term that converts units of phytoplankton density to nutrient concentration ((1000·µmol)·cell^{-1}). The parameters of the Monod equation, μ_{max} and K_S , can be considered as 'functional traits' that characterise a species' nutrient physiology. These traits have been shown to vary among species and play an important role in shaping competitive dynamics in phytoplankton communities. Furthermore, μ_{max} and K_S , are likely to exhibit temperature dependence. We expect maximum growth rate to be tightly coupled to metabolism, and consequently the temperature dependence of μ_{max} is expected to follow a left-skewed unimodal function of

temperature, where rates increase exponentially to an optimum followed by a steeper exponential decline. The effects of temperature on K_S are poorly understood and empirical studies have documented a wide range of temperature dependence functions (Aksnes & Egge 1991; Sterner & Grover 1998; Carter & Lathwell 1967; Mechling & Kilham 1982; Senft *et al.* 1981). The joint effects of temperature and nutrient concentrations on phytoplankton growth can be described by,

Then need some text emphasising how different spp, might differ in mu & Ks and their respective temperature sensitivities.

A model for the dynamics of two species competing for a single limiting resource at a range of temperatures would be

$$\frac{1}{N_a}\frac{dN_a}{dt}=\mu_a=\frac{\mu_{\max,a}S}{K_{S,a}+S}$$

$$\frac{1}{N_b}\frac{dN_b}{dt}=\mu_b=\frac{\mu_{\max,b}S}{K_{S,b}+S}$$

$$\frac{dS}{dt}=-\alpha_a N_b\frac{\mu_{\max,a}S}{K_{S,a}+S}-\alpha_b N_b\frac{\mu_{\max,b}S}{K_{S,b}+S}$$

would be great to show here how competitive outcomes depend on mismatches in traits by S and T.

Where the underscripts $_a$ and $_b$ denote of the identity of each species. In a scenario where species colonise a novel experiment, the competition starts when the two species are rare. In this situation, we hypothesise that differences in exponential growth (and therefore differences in the traits and variables that give rise to this growth rate) are key, whereas other mechanisms that might be more relevant once populations reach a carrying capacity, such as inter and intraspecific competition, might here play a minor role. Further, we assume that species only compete for a common resource. We hypothesise that competition will be driven by differences, or mismatches, in individual species' nutrient physiology traits, and that competitive outcomes are not significantly affected by direct interspecific interference such as production of toxins or competition for light. Finally, we neglect mortality rate. In this scenario, when the concentration of nutrients S is important, the growth rate of the two species μ_a and μ_b is close to $\mu_{\max}$. Therefore the competitive outcome between the two species is mainly driven by mismatches in the maximum growth rate, and species a wins when $\mu_{\max,a}>\mu_{\max,b}$. However, when S becomes lower, the importance of the half-saturation constant K_S becomes higher as it limits growth rate. A species having a lower K_S will be able to have a higher growth rate at low nutrient concentrations, thus species a will win when $K_{S,a}<K_{S,b}$.

Methods

Study design

We used an experimental approach to test the predictive ability of this simple competition model in predicting competitive outcomes in a context of climate change using 6 species of freshwater phytoplankton. We first determined species nutrient physiology traits μ_{max} and K_S and their temperature dependence. We then competed the 6 species in all pairwise combinations at two temperature and two nutrient levels. The results from the competition experiment where then matched to the models predictions, using the empirical data on species nutrient physiology to parametrize the model. The model is simple and explicitly only captures the traits and variables measured experimentally, except for the biomass conversion parameter, α. We therefore ran models with both a fixed α for all species (results largely robust to the choice of value), and with α_i proportional to median cell size, assuming that species with larger cell sizes would equate to a greater amount of phosphate per cell. The results are largely insensitive to the choice of α (indeed, species were initially chosen to be similar in size). Therefore, the results here are presented for a constant $\alpha = 1 \cdot 10^{-4}$. If the model were to predict correctly competitive outcomes, it would show that mismatches between traits have a great importance for species competition. Conversely, if the predictive power was low, it could suggest that mismatches in nutrient physiology alone are not the most important driver of the competition, and that other factors, and more complex models that include factors such as interspecific interference and density dependent growth need to be taken into account.

Species and culture conditions

The experiment was conducted with six species of freshwater green algae that are known to naturally co-occur, *Ankistrodesmus nannoselene, Chlamydomonas moewusii, Chlorella sorokiniana, Monoraphidium minutum, Scenedesmus obliquus* and *Selenastrum capricornutum* (Fritschie *et al.* 2014). We chose these 6 species because (i) they are similar cell size and (ii) can be cultured on the same media (e.g. standard COMBO culture medium without animal trace elements (Kilham *et al.* 1998)). Strains of each species were ordered in October 2015 from the Culture Collection of Algae and Protozoa (www.ccap.ac.uk, see Supplementary Table 1 for detailed information about the strains). Upon arrival, species were grown on COMBO culture medium, and maintained in semi-continuous culture in an Aralab incubator at 15°C on a 12:12 light-dark cycle with a light intensity of 90 µmol·m^{-2}·s^{-1}.

Nutrient and temperature dependence of growth rate

We measured growth rates of the 6 species of green algae across gradients in temperature and phosphate concentration. Each of the 6 species was grown in a factorial experiment at 5 temperatures and 13 phosphate concentrations, with 3 replicates per combination, amounting to a total of 1170 cultures. We created 13 solutions of different phosphate concentrations ranging from 0.01 µmol·L^{-1} of phosphate to 50 µmol·L^{-1} of phosphate (original phosphate concentration in the COMBO medium) by mixing different amounts of COMBO medium with and without potassium phosphate dibasic (Table S1B). This range was relevant to phosphate concentrations commonly found in lakes (Downing *et al.* 2001). Small tissue culture flasks (Nunclon) filled with 40 mL of each solution were inoculated with each species in monoculture with around 100 cells·mL^{-1}. Samples were diluted or concentrated by

filtration to allow for the same inoculation volume, 10 µL (for the very low phosphate concentrations, 0.01, 0.1 and 0.5 µmol·L^{-1}) and 50 µL (for all of the other samples), ensuring that the increase in phosphate concentration due to the inoculum was minimal (respectively 0.01 and 0.06 µmol·L^{-1}). Samples were then grown in Percival incubators at 15, 20, 25, 30, and 35°C on a 12:12 light-dark cycle and with a light intensity of 90 µmol·m^{-2}·s^{-1} (range: 70-110). Every day, samples were shaken and their position inside of the incubators was randomly changed. Every two days, a 200 µL sample was taken and 10 µL of 1% sorbitol solution was added as a cryoprotectant. After one hour of incubation in the dark, samples were frozen at -80°C until further analysis. Cell density in each sample was determined by flow cytometry (BD Accuri C6). Plates were thawed in a water bath at *ca* 38°C for 10 minutes and then run on the flow cytometer on fast flux settings (66 µL·min^{-1}), counting 10 µL of each sample. Cleaning fluid was run after each species to avoid contamination of measurements between species. The experiment was run for one month. During the experiment, some samples failed to grow properly and were therefore removed from the subsequent analyses.

Species competition

To investigate the joint effects of temperature and phosphate availability on competitive outcomes among the 6 species of algae, we competed each of the species in all pairwise combinations (15 pairs) at two temperatures (15 and 25°C; low temperature and a temperature close to the optimum for most species) and two phosphate concentrations (saturating [30 µmol·L^{-1}] and limiting [1 µmol·L^{-1}] concentrations, chosen from the Monod curves, see Fig. 1, Fig. S1), each replicated 6 times. We also grew the 6 species in monoculture at the two temperature and nutrient levels. The monoculture trials were divided into two subsets, one training subset, used to train the cell discrimination algorithm, which was replicated 3 times per temperature and nutrient levels and inoculated with 200 cells cells·mL^{-1}, and a testing subset used to test the accuracy of the cell discrimination algorithm, which was replicated 6 times per temperature and phosphate level and inoculated with 100 cells cells·mL^{-1}. In total, the design included 576 samples. The competition experiment was done in twenty-four 24 well plates filled with 2 mL of media, and inoculated with 100 or 200 cells·mL^{-1} of each species. The position of the species pairs were randomised within the plates, however given the large number of samples and to minimise experimenter error, we separated low-P from high-P plates. Plates were covered with AeraSeal breathable membrane, minimising evaporation and contamination but allowing gas exchange. The competition plates were incubated in the same way as described above for the monoculture growth curves. After 14 days, which was identified from the monoculture experiments as being sufficient time to reach stationary phase, a 200 µL sample was taken and preserved in the same way as described above. Cell density in each sample was determined by flow cytometry (BD Accuri C6) on the slow flux setting (14 µL·min), counting 20 µL of each sample. Cleaning fluid was run after each sample to avoid contamination of measurements between samples.

Data analyses

All statistical analyses were undertaken using R v3.3.2 (R Core Team 2014).

Nutrient and temperature dependence of growth rate

To characterise the effects of phosphorous availability and temperature on growth we estimated specific growth rate for each of the 1170 combinations of species, phosphate and temperatures from the time-series of cell densities. Population dynamics were fitted to the Buchanan three-phase linear growth model (Buchanan *et al.* 1997) using non-linear least squares regression.

$$N_t = \begin{cases} ¿\, N_0 \text{ for } t \le t_{lag}, \\ ¿\, N_0 + \mu(t - t_{lag}) \text{ for } t_{lag} < t < t_{max} \\ ¿\, N_t = N_{max} \text{ for } t \ge t_{max}, \end{cases} \quad \text{(x)}$$

where t_{lag} is the duration of the lag phase (days), t_{max} is the time when the maximum population density is reached (days), N_0 is the $\log_{10}$ of the initial population density ($\log_{10}$(cells·mL^{-1})), N_{max} is the $\log_{10}$ of the maximum population density supported by the environment ($\log_{10}$(cells·mL^{-1})), and μ is the specific growth rate (day^{-1}). Fits to the Buchanan model were determined using the 'nlsLM' function in the 'minpack.lm' package in R (Elzhov *et al.* 2010), which uses the Levenberg-Marquardt optimisation algorithm. Parameter estimation was achieved by running 1000 different random combination of starting parameters picked from uniform distributions and returning the parameter set with the lowest AICc score.

The Monod equation (Eq 1, Monod 1949), was fitted to the estimates of μ for each species at each temperature and for each of the three replicates using the 'nlsLM' function in the 'minpack.lm' package. Parameter estimation was achieved by running 1000 different random combination of starting parameters picked from a uniform distribution and returning the parameter set that returned the lowest AICc score.

We used generalized additive models (GAMs) to describe the thermal variation in μ_{max} and K_S. For each species, we fitted a gam model of each parameter with temperature as a smoother term with the number of knots fixed at 3 with the gam function from the mgcv package.

Competition

FSC files returned by the flow cytometer were read into R using the Bioconductor package 'FlowCore', returning side scatter (SSC), forward scatter (FSC), green fluorescence (FL1), orange fluorescence (FL2), red fluorescence (FL3), and blue fluorescence (FL4) values that could be used to define species morphology and thus discriminate between species in pairwise competition samples and determine species identity for each cell. We first filtered the data to remove noise by removing every data point where either ln(FSC.H)<10.3, ln(SSC.H)<3 or ln(FL3.H)<1.5, which are below minimum values observed for life cells of all species. We then separated the data set into 3 data frames, one for the isolates inoculated at 100 cells·mL^{-1}, and one for the isolates inoculated at 200 cells·mL^{-1}, and one for the competing species. The 200 cells·mL^{-1} isolates dataset measured at day 14 was used to determine pairwise discrimination functions between pair of species. We first removed outliers from this dataset by manually inspecting FSC.H by FL3.H clustering plots and choosing visual thresholds for these two values for each species. We then applied 3 different procedures to discriminate between pairs of species for each temperature and phosphate level: a linear discriminant analysis with the 'lda' function from the 'MASS' R package, a random forest analysis with the 'randomForest' function from the 'randomForest' R package and a recursive partitioning and regression tree analysis with the 'rpart' function from the 'rpart' R package. These analyses were performed using the natural logarithm of the 10 morphological variables returned by the flow cytometer (that is FSC.H, FSC.A, SSC.H, SSC.A, FL1.H, FL1.A, FL2.H, FL2.A, FL3.H, FL3.A, FL4.H and FL4.A, .H standing for height and .A for area), on each of the 15 pairs of species for each combination of temperature and phosphate

level. These different discriminant functions were then applied to the 100 cells·mL^{-1} isolates dataset previously filtered by removing visually determined outliers to test the accuracy of the predictions for the different discriminant methods. We then chose the method that gave the maximum level of accuracy to apply to the competition dataset (Fig. S2A). The best method was the linear discriminant analysis that gave 84 % of accuracy in predicting species identity (Table S2A).

After determining species identity for each sample, we computed cell density and calculated competition coefficients as the proportion of cells from the focal species over the total number of cells. We also computed a binary competition outcome where the competitive dominant was defined as the species that attained more than 50% of the total number of cells.

Results

Nutrient and temperature dependence of growth rate

The responses of growth rate to the gradients in phosphate concentration were well fit by the Monod equation (Fig. 1a). The half-saturation constant, K_S , and the maximum growth rate, μ_{max} , varied with temperature, and the temperature response of these traits differed between the 6 species (Table S3A and S3B). Maximum growth rate exhibited a unimodal temperature dependence in *Ankistrodesmus*, *Chlamydomonas*, and *Selenastrum* (Fig 1b, Table S3A). In *Chlorella* and *Monoraphidium*, μ_{max} increased monotonically and did not reach their optima by 35°C, while *Scenedesmus* exhibited negligible temperature dependence (Fig 1b, Table S3A). K_S increased with temperature for *Ankistrodesmus* and *Chlamydomonas*, while *Chlorella* and *Selenastrum* exhibited a unimodal response to temperature and there was no discernible trend for *Monoraphidium* and *Scenedesmus* (Fig. 1c, Table S3B). μ_{max} and K_S were also positively correlated (Pearson r = 0.45 [0.27,0.60], t = 4.77, df = 88, p <0.001), highlighting a trade-off between maximum growth rate and performance at low nutrient concentrations.

Species competition

Competition between species varied depending on temperature, nutrient conditions and pair identity (Fig. 2). For instance, for the pair *Chlorella-Ankistrodesmus*, *Chlorella* dominated the competition at low temperature, while *Ankistrodesmus* dominated at high temperature under both nutrient conditions. For the pair *Monoraphidium-Chlorella*, *Monoraphidium* won in every instance except at high nutrient concentration and high temperature, where *Chlorella* won. For the pair *Scenedesmus-Chlamydomonas*, at low temperature, there was no clear winner between the two species regardless of nutrient conditions, while at high temperature the outcome depended of nutrient conditions: at low nutrient conditions, there was no clear winner while at high nutrient conditions *Chlamydomonas* won (Fig. 2).

Differences in in μ (the realised growth rate estimated at the specific temperature and nutrient concentration) between the two competitors alone predicted the correct competitive outcome 62% of times (that is, the competitor with the higher μ won the competition; Table 2). Mismatches in μ_{max} (maximum growth rate at saturating nutrient concentrations from the Monod model) predicted the competitive outcome 60% of times, and differences in K_S only predicted the correct competitive outcome 37% of times (i.e., the competitor with the lower K_S won the competition). The difference in predictive power of mismatches in μ_{max} and K_S stands to reason given the positive correlation between individuals'

μ_{max} and K_S; given a high μ_{max} is associated to a high K_S, both μ_{max} and K_S are unlikely to equally be able to predict the outcome of a competition. The competition model, which incorporates both mismatches in μ_{max} and K_S, predicted the correct competitive outcome 65% of times. Therefore, the inclusion of both mismatches allowed for a marginally greater predictive power. Results remained largely the same when looking at the two temperatures and nutrient concentrations separately, but the predictability of the competitive outcome was very dependent on the species involved (Table 2). Competitions involving *Selenastrum* were considerably more difficult to predict with any of the mismatches (Table 2). This could, in part, be due to the lesser power of discrimination between cells in pairs involving this species (Table S2A), as well as to the wide confidence intervals around μ_{max} and K_S for this species (Fig 1). Indeed, only removing competitions involving *Selenastrum* increased the predictive power of mismatches in μ, μ_{max} and the competition model (72.5%, 72.5%, and 77.5% of outcomes correctly predicted, respectively) but not that of mismatches in K_S (32.5%). The results were robust to the statistical method used to calculate μ_{max} and K_S, as well as to the statistical method used to discriminate between species (Supplementary material S7).

The results indicate that μ_{max} is a distinctly more important trait for predicting competitive outcomes than is K_S, suggesting that performance at low nutrient concentrations had little bearing in a species' competitive ability. Simulations clearly show that at higher nutrient concentrations, mismatches in K_S have little or no influence on competitions (Fig. 3a, c). At the lower nutrient concentration, mismatches in K_S are of greater importance, but mismatches in μ_{max} nonetheless still dominate (Fig. 3b, d).

In some cases, the winner of a competition changed depending on the nutrient concentration and/or temperature. For example, *Chlorella* won against *Chlamydomonas* at 15°C, but the reverse was true at 25°C. These reversals, or flips of the competitive outcome, were far more likely to occur between temperatures (in 18 out of 30 competitions; 15 pairs and two nutrient concentrations) than between nutrient concentrations (six out of 30). In the 18 reversals due to the change in temperature, 14 coincided with similar reversals in the species' μ_{max} (i.e., μ_{max} was higher for one species at one temperature, but not at the other), and only six coincided with reversals in species' K_S, thus corroborating the greater significance of μ_{max} in determining competitive outcomes (Table 2).

Discussion

Global change is predicted to affect both the temperature of aquatic ecosystems (IPCC 2013) and their nutrient balance (e.g. through an increase in vertical stratifications, reducing nutrient supply (Behrenfeld *et al.* 2006), or through an increase in eutrophication, increasing nutrient supply (Ye *et al.* 2011)). These shifts could lead to mismatches between competing species' physiological traits, and influence the outcome of the competition. Here we showed that phytoplankton species varied for their temperature response of nutrient physiology traits, and that this variation affected competition between species. Mismatches between species maximum growth rate μ_{max} and/or between species half-saturation constant K_S led to reversals in competitive outcome between pairs of species depending on environmental conditions.

We found that traits governing species nutrient physiology were not fixed values for a species but varied plastically with temperature. Growth rate depended both on temperature and nutrients non-linearly for each species. Half-saturation constants generally increased with temperature. These results are in accordance with previous results showing a positive relationship between K_S and temperature in plants (Carter & Lathwell 1967) or in algae for nitrogen (Aksnes & Egge 1991; Sterner & Grover 1998) and silicate (Mechling & Kilham 1982), and a hump shaped relationship between Ks and temperature in algae for phosphorus (Senft *et al.* 1981). Studies investigating effects of climate change on algal biomass often consider the half-saturation constant to be independent of temperature (Goldman & Carpenter 1974; Ye *et al.* 2011; Thomas *et al.* 2017); our results highlight the temperature-dependence of nutrient-limited growth. Further, the relationship between temperature and nutrient physiology depended on species identity, with for instance *Selenastrum* having a much higher half-saturation constant than *Ankistrodesmus*.

Competitive outcomes between pairs of species varied with temperature and nutrient conditions. These results match previous studies, where temperature has been shown to influence competitive interactions in various groups including phytoplankton, arthropods and vertebrates (see (Dunson & Travis 1991) for a review). Mismatches in nutrient uptake traits were a good predictor of competitive outcomes between species. Particularly, mismatches in μ_{max} were clearly a better predictor of competitive ability than performance at low nutrient concentrations, although knowledge of mismatches in both traits using the model helped improve predictive power. Our results in fact indicate that μ_{max} was the more important trait even at low nutrient concentrations, when we would have expected K_S to be most significant (Table 2, Figure 3). This could be due to the relatively large confidence intervals around our estimates of K_S, or to the fact that the lowest concentration of phosphate used in the competition experiment, 1 µmol·L^{-1}, was still relatively high compared to the half-saturating constant of most species. Our results on the predictability of competitive outcomes (Table 2) should also be interpreted in the context that competitions were very variable across replicates (Figure 2), that is to say, both competing species were often observed to win across six replicates. Competitive outcomes were highly predictable when excluding competitions involving *Selenastrum*, suggesting that the other species predominantly compete for resources (and implying that there is little direct interference). On the other hand, the predictability of *Selenastrum*'s competitive outcomes was poor. This might have been due to the fact that our discriminating power for this species was low (Table S2Ab), but could also indicate that competitions with this species might have involved some significant form of direct interspecific interference (e.g. production of toxins), as also indicated by the fact that competitive interactions involving this species were all strongly negative, leading to a strongly diminished yield of the pair of competitors relative to the same species in monoculture (Loreau & Hector 2001) deviation from expected yield in pairs involving the focal species, mean ± SD, -0.77 ± 0.36 in pairs involving *Selenastrum*, compared to -0.37 ± 0.64, -0.13 ± 0.51, -0.19 ± 0.72 and -0.23 ± 0.53 in pairs involving *Ankistrodesmus*, *Chlamydomonas*, *Chlorella*, *Monoraphidium* and *Scenedesmus* respectively).

We highlighted different competitions where some species always won, while there were frequent reversals of competitive outcomes, particularly with temperature and less so with nutrients. Reversals in competitive outcomes were often linked to analogous reversals in the values of μ_{max}. Mismatches in both μ and μ_{max} were themselves linked to mismatches in physiological traits. Therefore having a better understanding on the thermal-dependency of species nutrient physiology is an important step if we are to understand how species competition and community functioning can be affected by climate change (Litchman

& Klausmeier 2008; Litchman *et al.* 2010). The results of our study contrast with some earlier studies, as (Park 1954) found that higher growth rate of a competitor at higher temperature did not lead to a switch in competitive dominance in *Tribolium* species.

More generally, our findings stress the importance of considering how species traits will plastically change with temperature to better understand biotic interactions in a context of global climate change. Studying consequences of climate change in terms of mismatches between physiological traits should be a useful approach in understanding how species interactions will be modified by warming climates (Dell *et al.* 2014). Further, because global changes are unlikely to act only through temperature changes but should involve rapid modifications of both nutrient and thermal conditions (Behrenfeld *et al.* 2006; Ye *et al.* 2011; IPCC 2013), it is crucial to better understand how the combination of multiple stressors should affect species and community responses to global changes. We highlight the interest of considering a spectrum of different ecological contexts to predict successful competitors and invaders, and to pinpoint which mismatch in species traits is more important in which ecological context.

Acknowledgements: We thank Saskia Johnson and Emily Budd for their help in the experiments. This work was supported by a NERC grant number XXXXXX to GYD and SP.

References

1. Aksnes, D.L. & Egge, J.K. (1991). A theoretical model for nutrient uptake in phytoplankton. *Marine Ecology Progress Series*, 70, 65–72

2. Amarasekare, P. (2015). Effects of temperature on consumer–resource interactions. *J Anim Ecol*, 84, 665–679

3. Behrenfeld, M.J., Boss, E., Siegel, D.A. & Shea, D.M. (2005). Carbon-based ocean productivity and phytoplankton physiology from space. *Global Biogeochem. Cycles*, 19, GB1006

4. Behrenfeld, M.J., O'Malley, R.T., Siegel, D.A., McClain, C.R., Sarmiento, J.L., Feldman, G.C., *et al.* (2006). Climate-driven trends in contemporary ocean productivity. *Nature*, 444, 752–755

5. Bellard, C., Bertelsmeier, C., Leadley, P., Thuiller, W. & Courchamp, F. (2012). Impacts of climate change on the future of biodiversity. *Ecology Letters*, 15, 365–377

6. Bestion, E. & Cote, J. (2017). Species Responses to Climate Change: Integrating Individual-Based Ecology Into Community and Ecosystem Studies. In: *Reference Module in Earth Systems and Environmental Sciences*. Elsevier

490
4917.
492Brown, J.H., Gillooly, J.F., Allen, A.P., Savage, V.M. & West, G.B. (2004). Toward a metabolic theory of
493ecology. *Ecology*, 85, 1771–1789
494
4958.
496Buchanan, R.L., Whiting, R.C. & Damert, W.C. (1997). When is simple good enough: a comparison of
497the Gompertz, Baranyi, and three-phase linear models for fitting bacterial growth curves. *Food*
498*Microbiology*, 14, 313–326
499
5009.
501Bulgakov, N.G. & Levich, A.P. (1999). The nitrogen : Phosphorus ratio as a factor regulating
502phytoplankton community structure : Nutrient ratios. *Archiv für Hydrobiologie*, 146, 3–22
503
50410.
505Cahill, A.E., Aiello-Lammens, M.E., Fisher-Reid, M.C., Hua, X., Karanewsky, C.J., Ryu, H.Y., *et al.* (2013).
506How does climate change cause extinction? *Proc. R. Soc. B*, 280, 20121890
507
50811.
509Carter, O.G. & Lathwell, D.J. (1967). Effects of Temperature on Orthophosphate Absorption by Excised
510Corn Roots. *Plant Physiol.*, 42, 1407–1412
511
51212.
513Dell, A.I., Pawar, S. & Savage, V.M. (2011). Systematic variation in the temperature dependence of
514physiological and ecological traits. *PNAS*, 108, 10591–10596
515
51613.
517Dell, A.I., Pawar, S. & Savage, V.M. (2014). Temperature dependence of trophic interactions are
518driven by asymmetry of species responses and foraging strategy. *J Anim Ecol*, 83, 70–84
519
52014.
521Downing, J.A., Watson, S.B. & McCauley, E. (2001). Predicting Cyanobacteria dominance in lakes.
522*Can. J. Fish. Aquat. Sci.*, 58, 1905–1908
523
52415.
525Dunn, R.R., Harris, N.C., Colwell, R.K., Koh, L.P. & Sodhi, N.S. (2009). The sixth mass coextinction: are
526most endangered species parasites and mutualists? *Proc. R. Soc. B*, 276, 3037–3045
527
52816.
529Dunson, W.A. & Travis, J. (1991). The Role of Abiotic Factors in Community Organization. *The*
530*American Naturalist*, 138, 1067–1091
531
53217.
533Elzhov, T.V., Mullen, K.M. & Bolker, B. (2010). R interface to the Levenberg-Marquardt nonlinear least-
534squares algorithm found in MINPACK
535
53618.
537Field, C.B., Barros, V.R. & Intergovernmental Panel on Climate Change (Eds.). (2014). *Climate change*
538*2014: impacts, adaptation, and vulnerability: Working Group II contribution to the fifth assessment*
539*report of the Intergovernmental Panel on Climate Change*. Cambridge University Press, New York, NY

540
54119.
542Fritschie, K.J., Cardinale, B.J., Alexandrou, M.A. & Oakley, T.H. (2014). Evolutionary history and the
543strength of species interactions: testing the phylogenetic limiting similarity hypothesis. *Ecology*, 95,
5441407–1417
545
54620.
547Gilbert, B., Tunney, T.D., McCann, K.S., DeLong, J.P., Vasseur, D.A., Savage, V., *et al.* (2014). A
548bioenergetic framework for the temperature dependence of trophic interactions. *Ecol Lett*, 17, 902–
549914
550
55121.
552Goldman, J.C. & Carpenter, E.J. (1974). A kinetic approach to the effect of temperature on algal
553growth. *Limnology and Oceanography*, 19, 756–766
554
55522.
556Grover, J.P. & Chrzanowski, T.H. (2006). Seasonal dynamics of phytoplankton in two warm temperate
557reservoirs: association of taxonomic composition with temperature. *J Plankton Res*, 28, 1–17
558
55923.
560IPCC. (2013). *Climate change 2013: the physical science basis : Working Group I contribution to the
561fifth assessment report of the Intergovernmental Panel on Climate Change*. Cambridge University
562Press, Cambridge, United Kingdom and New York, NY, USA
563
56424.
565Kilham, S.S., Kreeger, D.A., Lynn, S.G., Goulden, C.E. & Herrera, L. (1998). COMBO: a defined
566freshwater culture medium for algae and zooplankton. *Hydrobiologia*, 377, 147–159
567
56825.
569Kingsolver, J.G. (2009). The Well-Temperatured Biologist. *The American Naturalist*, 174, 755–768
570
57126.
572Kordas, R.L., Harley, C.D.G. & O'Connor, M.I. (2011). Community ecology in a warming world: The
573influence of temperature on interspecific interactions in marine systems. *Journal of Experimental
574Marine Biology and Ecology*, Global change in marine ecosystems, 400, 218–226
575
57627.
577Litchman, E. & Klausmeier, C.A. (2008). Trait-Based Community Ecology of Phytoplankton. *Annual
578Review of Ecology, Evolution, and Systematics*, 39, 615–639
579
58028.
581Litchman, E., Pinto, P. de T., Klausmeier, C.A., Thomas, M.K. & Yoshiyama, K. (2010). Linking traits to
582species diversity and community structure in phytoplankton. *Hydrobiologia*, 653, 15–28
583
58429.
585Loreau, M. & Hector, A. (2001). Partitioning selection and complementarity in biodiversity
586experiments. *Nature*, 412, 72–76
587
58830.
589Magozzi, S. & Calosi, P. (2015). Integrating metabolic performance, thermal tolerance, and plasticity

590enables for more accurate predictions on species vulnerability to acute and chronic effects of global
591warming. *Global Change Biology*, 21, 181–194
592
59331.
594Mechling, J.A. & Kilham, S.S. (1982). Temperature Effects on Silicon Limited Growth of the Lake
595Michigan Diatom Stephanodiscus Minutus (bacillariophyceae)1. *Journal of Phycology*, 18, 199–205
596
59732.
598Monod, J. (1949). The growth of bacterial cultures. *Annual Reviews in Microbiology*, 3, 371–394
599
60033.
601O'Connor, M.I., Gilbert, B. & Brown, C.J. (2011). Theoretical Predictions for How Temperature Affects
602the Dynamics of Interacting Herbivores and Plants. *The American Naturalist*, 178, 626–638
603
60434.
605Pacifici, M., Foden, W.B., Visconti, P., Watson, J.E.M., Butchart, S.H.M., Kovacs, K.M., *et al.* (2015).
606Assessing species vulnerability to climate change. *Nature Clim. Change*, 5, 215–224
607
60835.
609Park, T. (1954). Experimental Studies of Interspecies Competition II. Temperature, Humidity, and
610Competition in Two Species of Tribolium. *Physiological Zoology*, 27, 177–238
611
61236.
613R Core Team. (2014). *R: A Language and Environment for Statistical Computing*. R Foundation for
614Statistical Computing, Vienna, Austria
615
61637.
617Reuman, D.C., Holt, R.D. & Yvon-Durocher, G. (2014). A metabolic perspective on competition and
618body size reductions with warming. *J Anim Ecol*, 83, 59–69
619
62038.
621Savage, V.M., Gillooly, J.F., Brown, J.H., West, G.B. & Charnov, E.L. (2004). Effects of Body Size and
622Temperature on Population Growth. *The American Naturalist*, 163, 429–441
623
62439.
625Senft, W.H., Hunchberger, R.A. & Roberts, K.E. (1981). Temperature Dependence of Growth and
626Phosphorus Uptake in Two Species of Volvox (volvocales, Chlorophyta)1. *Journal of Phycology*, 17,
627323–329
628
62940.
630Sterner, R.W. & Grover, J.P. (1998). Algal growth in warm temperate reservoirs: kinetic examination of
631nitrogen, temperature, light, and other nutrients. *Water Research*, 32, 3539–3548
632
63341.
634Thomas, C.D., Cameron, A., Green, R.E., Bakkenes, M., Beaumont, L.J., Collingham, Y.C., *et al.* (2004).
635Extinction risk from climate change. *Nature*, 427, 145–148
636
63742.
638Thomas, M.K., Aranguren-Gassis, M., Kremer, C.T., Gould, M.R., Anderson, K., Klausmeier, C.A., *et al.*
639(2017). Temperature–nutrient interactions exacerbate sensitivity to warming in phytoplankton. *Glob*
640*Change Biol*, n/a-n/a

641
64243.
643Thomas, M.K., Kremer, C.T. & Litchman, E. (2016). Environment and evolutionary history determine
644the global biogeography of phytoplankton temperature traits. *Global Ecology and Biogeography*, 25,
64575–86
646
64744.
648Tilman, D. (1981). Tests of Resource Competition Theory Using Four Species of Lake Michigan Algae.
649*Ecology*, 62, 802–815
650
65145.
652Tylianakis, J.M., Didham, R.K., Bascompte, J. & Wardle, D.A. (2008). Global change and species
653interactions in terrestrial ecosystems. *Ecology Letters*, 11, 1351–1363
654
65546.
656Uszko, W., Diehl, S., Englund, G. & Amarasekare, P. (2017). Effects of warming on predator–prey
657interactions – a resource-based approach and a theoretical synthesis. *Ecol Lett*, n/a-n/a
658
65947.
660Ye, C., Shen, Z., Zhang, T., Fan, M., Lei, Y. & Zhang, J. (2011). Long-term joint effect of nutrients and
661temperature increase on algal growth in Lake Taihu, China. *Journal of Environmental Sciences*, 23,
662222–227
663

664

Figures:

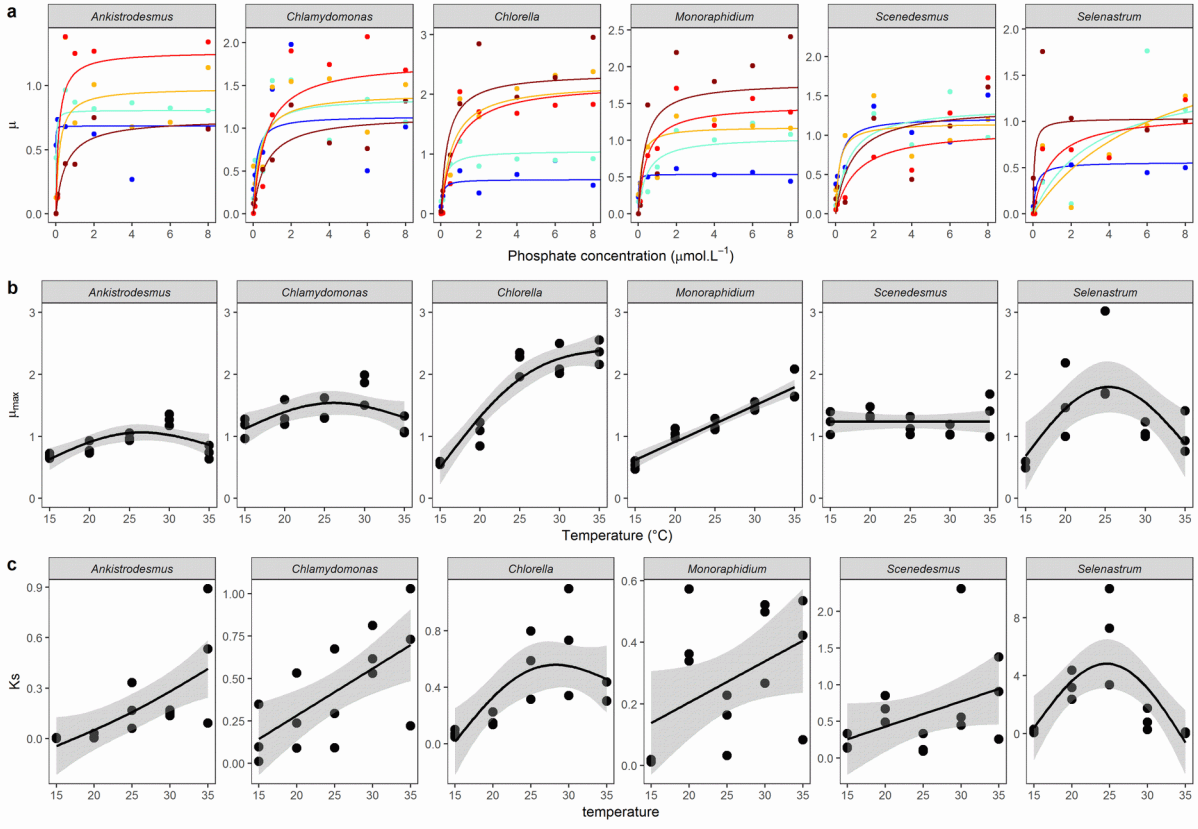

Fig 1:

(a) Mean Monod curves for each species growth rate. Growth rate μ as a function of phosphate concentration in the medium (µmol·L^{-1}) and temperature (from blue: 15°C to dark red: 35°C). Points represent the mean of the 3 replicates, and the Monod curve is drawn from the mean of the rate μ_{max} and K_S parameters from the 3 replicates. Note that the phosphate concentration levels in the experiment go from 0.01 to 50 µmol·L^{-1} but the x-axis was cut at 8 µmol·L^{-1} for clarity. **(b)** Half-saturation coefficient K_S and **(b)** Maximum growth rate μ_{max} as a function of temperature. **(c)** Half-saturation coefficient K_S Lines represent the fit of the GAM models investigating the temperature dependence of each parameter. See Tables S3A and S3B for more details about the temperature-dependence of the estimates from the Monod model.

680

681

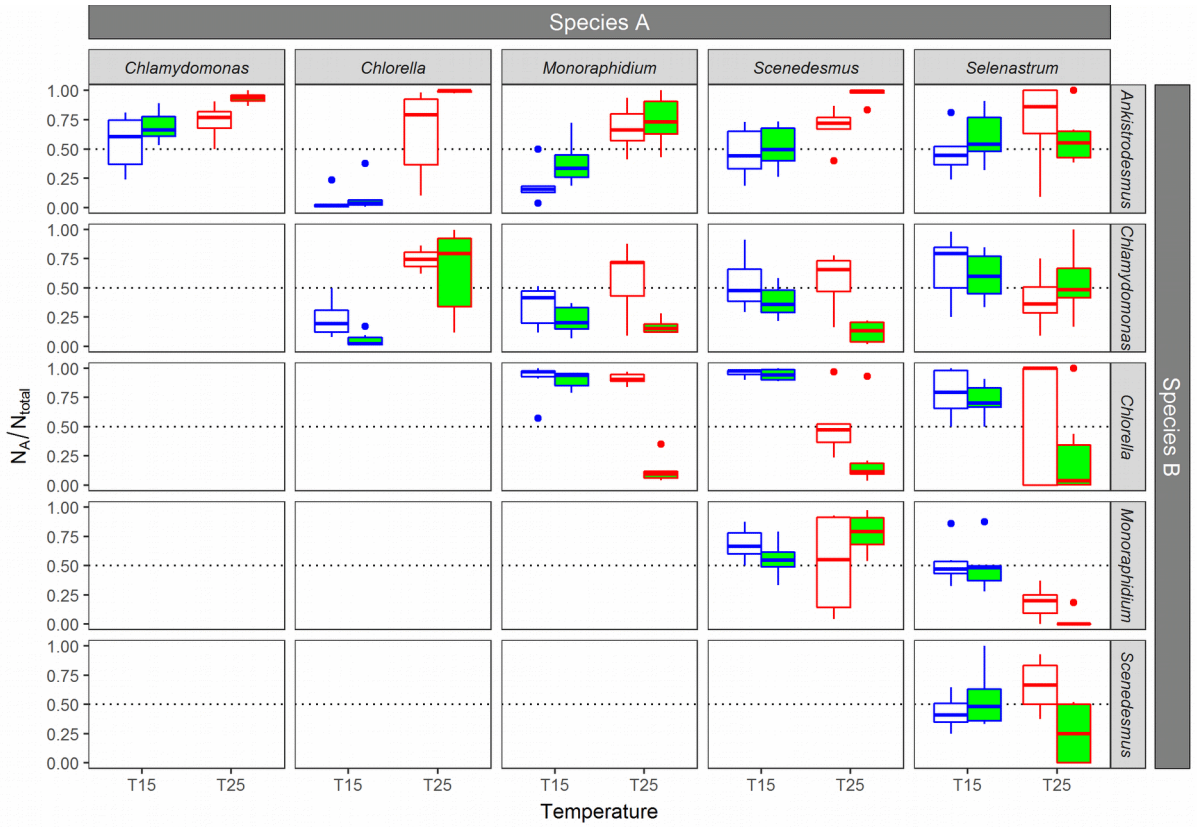

682

683**Fig. 2:**

684Competition between species. For each pair of species, the proportion of cells from species A
685over the total number of cells at day 14. Colours represent the temperature of the trial, blue:
68615°C, red: 25°C; and fills represent the nutrient conditions of the trial, white: non-saturated
687nutrient solution (1 µmol·L^{-1} of phosphate), green, saturated nutrient solution (30 µmol·L^{-1} of
688phosphate). Boxplots represent the values of the 6 replicates per condition. The dotted line
689represents the situation where 50% of the total number of cells pertain to the species A.

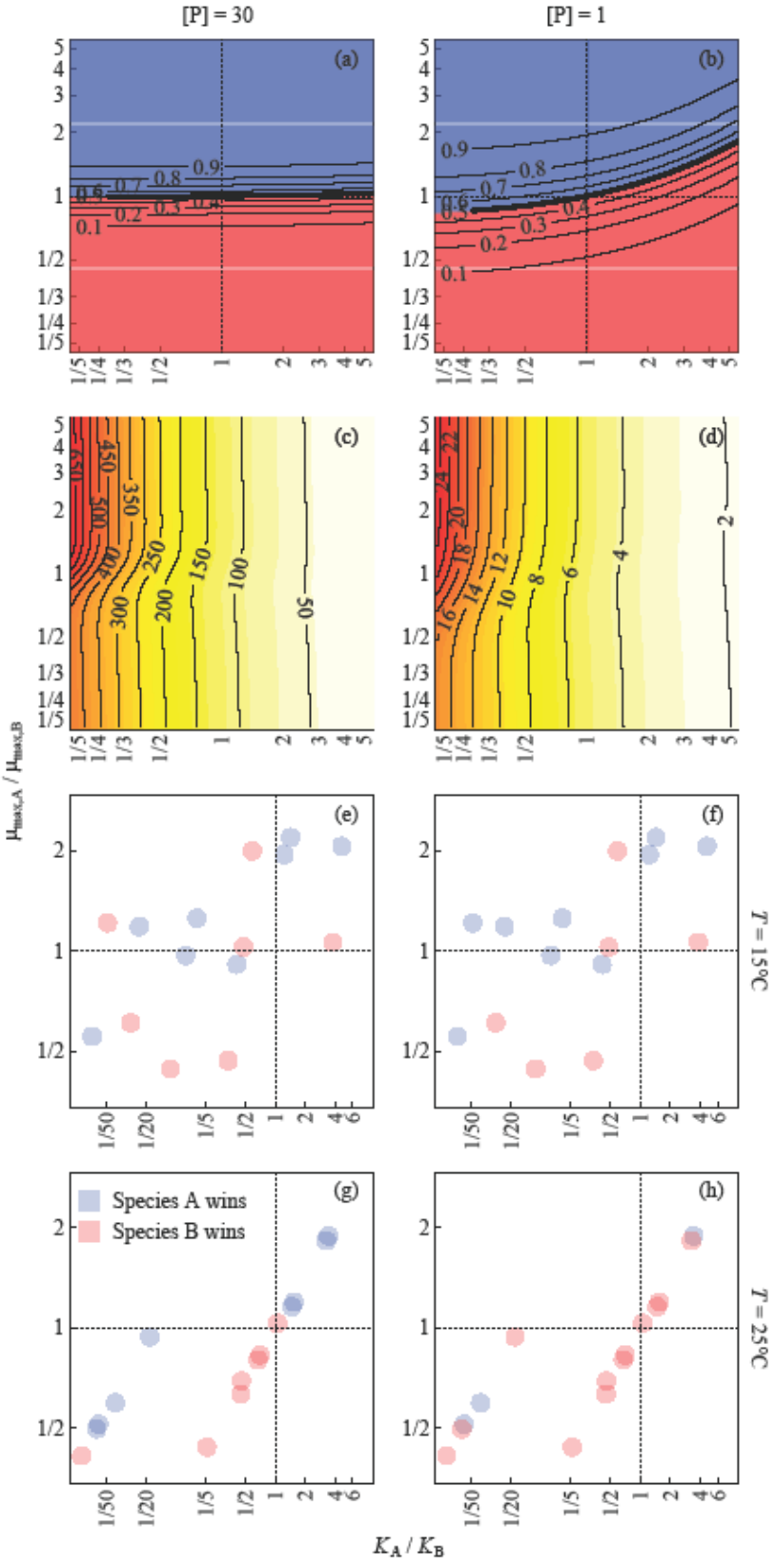

690

691**Fig 3:**

692 Relative importance of mismatches in μ_{max} and K_S in determining competitive 693outcomes. Panels (a, b) show the proportion of cells belonging to species A after 14 days 694according to the competition model, for a range of mismatches in both traits (see 695Supplementary Section S6 for details). Panels (c, d) show the relative importance of a small

696increase in the mismatches of the two traits on competitive outcomes. For example, a value of
69710 means that a small increase in the ln ratio of μ_{max} has a 10 times greater impact on the
698competitive outcome than does the same small increase in the ln ratio of K_S. Panels (e-h)
699show the equivalent experimental results for $T = 15$ °C (e, f) and 25°C (g, h), and
700competitive outcomes (colour of points) refer to the median of six replicates. Panels (a, c, e,
701g) are for a starting nutrient concentration of 30 µmol·L^{-1} and (b, d, e, f) are for a starting
702concentration of 1 µmol·L^{-1}. The legend in (g) applies to all panels except (c, d).

703

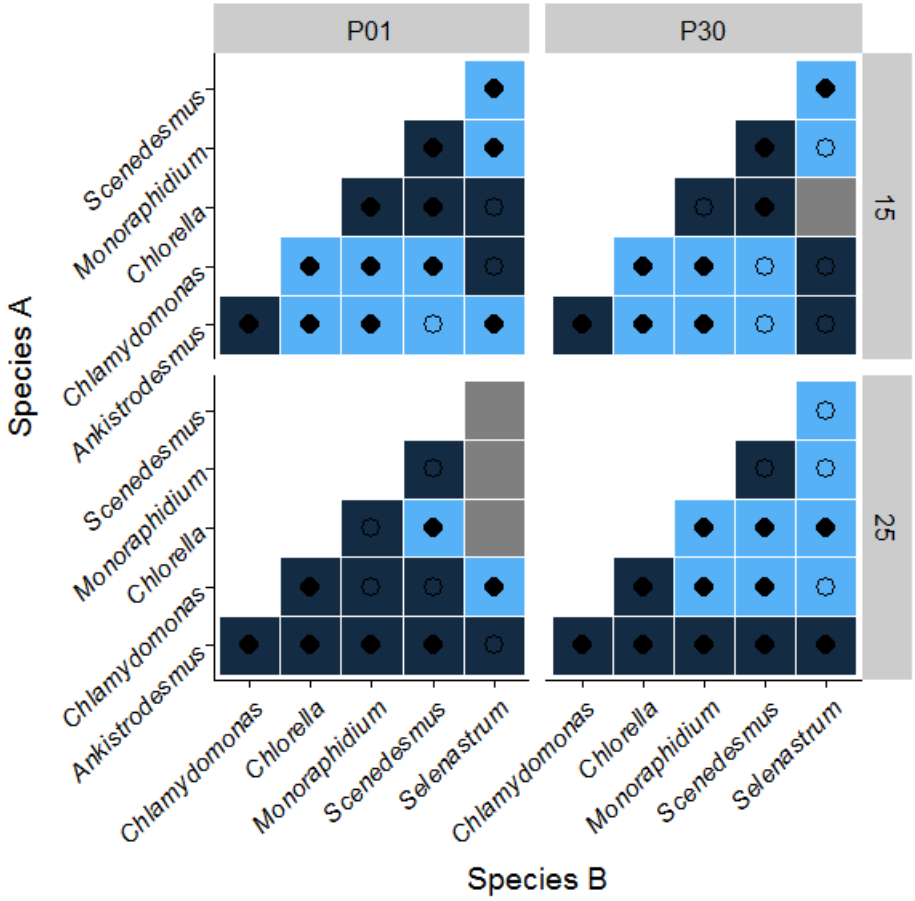

704

705

706Figure 4: Outcome of the competition and validity of the model predictions for each pair of
707species depending on the temperature and phosphate level. The color indicates the identity of
708the winning species (lightblue species A wins, darkblue species B wins), and the shape inside
709shows whether the model prediction is correct (filled, the model is correct, empty, the model
710is incorrect).

Tables

Table 1: Proportion of competitive outcomes correctly predicted by mismatches in individual photosynthetic capacity (rP158), in μ (the growth rate from the Buchanan model at each temperature and nutrient concentration combination), μ_{max} (maximum growth rate at saturating nutrient concentrations from the Monod model), K_S (where a lower K_S is assumed to be beneficial), and both μ_{max} and K_S (using the competition model), for all competitions, and by subsets (by temperature, by nutrient concentration, and by species where only competitions involving a specific species are included). Numbers in brackets show the proportion of 10,000 random runs with greater predictive power (see Supplementary Information Section S6). The experimental competition data uses the LDA discrimination method, and we here used the median value of the proportion of cells of a competitor across the six replicates. Monod model parameters (μ_{max} and K_S) are the parameter estimates from the mixed effects model described in Methods.

Subset	rP158	μ	μ_{max}	K_S	Model	N
Full dataset						
	0.70 (0.001)	0.62 (0.026)	0.60 (0.061)	0.40 (0.683)	0.65 (0.044)	60
By temperature						
$T = 15$ °C	0.80 (0.000)	0.67 (0.021)	0.57 (0.175)	0.43 (0.489)	0.67 (0.085)	30
$T = 25$ °C	0.60 (0.114)	0.57 (0.186)	0.63 (0.068)	0.30 (0.666)	0.63 (0.126)	30
By nutrient concentration						
$P = 1$ µmol·L^{-1}	0.70 (0.009)	0.57 (0.160)	0.60 (0.062)	0.43 (0.525)	0.67 (0.032)	30
$P = 30$ µmol·L^{-1}	0.70 (0.016)	0.67 (0.035)	0.60 (0.078)	0.37 (0.745)	0.63 (0.089)	30
By species						
Ankistrodesmus	0.90 (0.000)	0.45 (0.510)	0.85 (0.005)	0.35 (0.598)	0.80 (0.039)	20
Chlamydomonas	0.75 (0.006)	0.65 (0.046)	0.60 (0.114)	0.30 (0.769)	0.70 (0.046)	20
Chlorella	0.70 (0.059)	0.85 (0.003)	0.70 (0.087)	0.30 (0.698)	0.75 (0.087)	20
Monoraphidium	0.60 (0.077)	0.65 (0.027)	0.50 (0.241)	0.60 (0.061)	0.65 (0.068)	20
Scenedesmus	0.80 (0.000)	0.70 (0.004)	0.60 (0.059)	0.40 (0.553)	0.60 (0.125)	20
Selenastrum	0.45 (0.520)	0.40 (0.689)	0.35 (0.731)	0.45 (0.390)	0.40 (0.753)	20

Table2:

Link between competitive reversals and reversals in traits due to temperature. For each pair of species and each phosphate level, the sum of reversals observed in traits (μ_{max} and K_S) or competitive outcomes between 15 and 25°C. Out of the 18 competitive reversals observed between temperature levels, 8 were linked to reversals in μ_{max} alone, 6 were linked to reversals in both traits μ_{max} and K_S while 4 were not linked to any kind of reversals between nutrient physiology traits. For a more detailed description of the competitive outcomes, see Supplementary material S6

	Reversal in μ_{max}		**Reversal in K_S**		**Reversal in μ_{max} and K_S**	
Reversal in	Yes (N = 20)	No (N = 10)	Yes (N = 10)	No (N = 20)	Yes (N = 10)	No (N = 20)

competition						
Yes (N = 18)	14	4	6	12	6	12
No (N = 12)	6	6	4	8	4	8

735

736

Supplementary Information

S1: Experimental design

Figure S1A: Flow chart of the experimental design

Table S1A:

Detailed information about the 6 species

Species name	Class	Order	Strain	Origin
Ankistrodesmus nannoselene Skuja (1948)	Chlorophyceae	Sphaeropleales	CCAP 202/6A	Siggeforsajon, Sweden
Chlamydomonas moewusii Gerlof (1940)	Chlorophyceae	Chlamydomonadales	CCAP 11/5A	Freshwater
Chlorella sorokiniana Shihira & Krauss (1965)	Trebouxiophyceae	Chlorellales	CCAP 211/8K	Austin, Texas, USA
Monoraphidium minutum (Nägeli) Komarkova-Legnerova (1969)	Chlorophyceae	Sphaeropleales	CCAP 278/3	Texas, USA
Scenedesmus obliquus (Turpin) Kützing (1833)	Chlorophyceae	Sphaeropleales	CCAP 276/3B	Lund, Sweden
Selenastrum capricornutum Printz (1913)	Chlorophyceae	Sphaeropleales	CCAP 278/4	Akershus, Norway

Table S2A:

Phosphate concentration levels for each solution in µmol·L^{-1} and µg·L^{-1}. We created 13 solutions of different phosphate concentrations ranging from 0.01 µmol.L^{-1} of phosphate to 350 µmol.L-1 of phosphate by mixing different amounts of COMBO medium without potassium phosphate dibasic (P- COMBO) and normal COMBO medium (P+ COMBO) in 40 mL nunclons. We used a modified version of the standard COMBO medium without animal trace solution in which we increased the fraction of carbonate by adding 10 mL of a stock solution of 55.8 g. L^{-1} of sodium bicarbonate to maintain a DIC of more than 6.6 mmol.L^{-1} in order to prevent carbon limitation, which allowed a C:N:P ratio of 132:20:1 in the P+ COMBO solution, above the Redfield ratio of 106:16:1.

Phosphate concentration (µmol·L^{-1})	50	40	30	20	10	8	6	4	2	1	0.5	0.1	0.01
Phosphate concentration (µg·L^{-1})	4750	3800	2850	1900	950	760	570	380	190	95	47.5	9.5	0.95
Amount of P+ COMBO (mL)	40	32	24	16	8	6.4	4.8	3.2	1.6	0.8	0.4	0.08	0.008
Amount of P- COMBO (mL)	0	8	16	24	32	33.6	35.2	36.8	38.4	39.2	39.6	40	40

S2: Discrimination between species in the competition experiment

Table S2A:

A: Proportion of correct assignations for each discrimination method (LDA: linear discriminant analysis, Random Forest analysis, RPART: recursive partitioning and regression tree) summarised by phosphate and nutrient conditions for all pair of species. B: Proportion of correct assignations for each discrimination method summarised by pair of species for all nutrient and thermal conditions. C: Proportion of correct assignations for each discrimination method summarised by species for all nutrient and thermal conditions

A

Temperature	Nutrient	LDA	Random forest	RPART
15	1	0.79	0.68	0.64
15	30	0.85	0.8	0.76
25	1	0.7	0.69	0.68
25	30	0.64	0.66	0.62
Mean		**0.75**	**0.71**	**0.68**

B

Species	LDA	Randomforest	RPART
Ankistrodesmus	0.91	0.86	0.72
Chlamydomonas	0.93	0.93	0.81
Chlorella	0.85	0.86	0.67
Monoraphidium	0.84	0.78	0.65
Scenedesmus	0.83	0.77	0.61
Selenastrum	0.70	0.68	0.48
Mean	**0.84**	**0.81**	**0.66**

776C

Pair of species	LDA	Randomforest	RPART
Ankistrodesmus-Chlamydomonas	1	1	0.94
Ankistrodesmus-Chlorella	0.91	0.88	0.73
Ankistrodesmus-Monoraphidium	0.87	0.74	0.71
Ankistrodesmus-Scenedesmus	0.95	0.93	0.71
Ankistrodesmus-Selenastrum	0.82	0.73	0.52
Chlamydomonas-Chlorella	0.96	0.96	0.79
Chlamydomonas-Monoraphidium	0.96	0.97	0.86
Chlamydomonas-Scenedesmus	0.94	0.92	0.74
Chlamydomonas-Selenastrum	0.78	0.8	0.74
Chlorella-Monoraphidium	0.83	0.85	0.7
Chlorella-Scenedesmus	0.86	0.84	0.65
Chlorella-Selenastrum	0.67	0.76	0.48
Monoraphidium-Scenedesmus	0.88	0.69	0.63
Monoraphidium-Selenastrum	0.68	0.67	0.33
Scenedesmus-Selenastrum	0.53	0.46	0.34
Mean	**0.84**	**0.81**	**0.66**

777

778

779

780

781

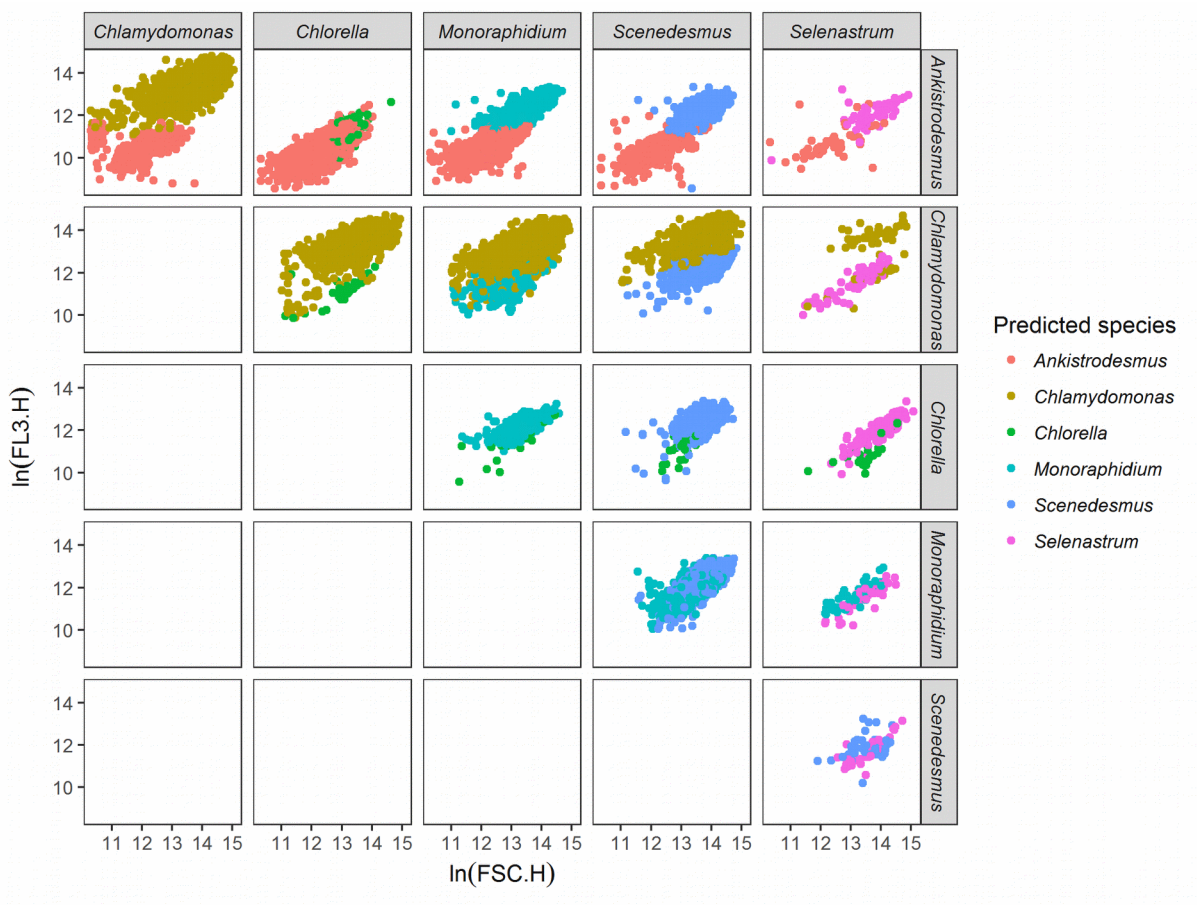

782

783**Figure S2A:**

784 Example of discrimination between species among pairs of species, here for species grown at
78515°C in saturating nutrient conditions after 14 days of experiment. Each dot represents a cell,
786here mapped on FSC.H (size proxy) and FL3.H (chlorophyll a proxy) characteristics from the
787flow cytometer. Colours represent the species predicted by the discrimination algorithm. The
788discrimination algorithm is a linear discriminant analysis trained with flow cytometer data
789(FSC.H, FSC.A, SSC.H, SSC.A, FL1.H, FL1.A, FL2.H, FL2.A, FL3.H, FL3.A, FL4.H, and
790FL4.A) from the species grown in isolates at the same temperature and nutrient conditions.
791For example, *Chlamydomonas* outcompetes *Chlorella* in these nutrient and temperature
792conditions.

793

S3: Temperature dependency of the estimates from the Monod model

Table S3A:
Results from the GAM models investigating μ_{max} as a function of temperature for each species. See Fig 1 for the representation of the GAM model.

Species	edf	F	p-value	R^2
Ankistrodesmus	2	6.74	0.011*	0.45
Chlamydomonas	2	3.42	0.066.	0.26
Chlorella	2	54.02	>0.001***	0.88
Monoraphidium	2	63.67	>0.001***	0.90
Scenedesmus	2	0.41	0.674	-0.09
Selenastrum	2	5.82	0.017*	0.41

Table S3B:
Results from the GAM models investigating K_S as a function of temperature for each species. See Fig 1 for the representation of the GAM model.

Species	edf	F	p-value	R^2
Ankistrodesmus	2	6.29	0.013*	0.43
Chlamydomonas	2	4.53	0.034*	0.34
Chlorella	2	6.37	0.013*	0.43
Monoraphidium	2	2.17	0.157	0.14
Scenedesmus	2	1.32	0.302	0.04
Selenastrum	2	7.92	0.006**	0.50

S5: Significance of competitive outcomes predicted by the model

To quantify the significance of the model's ability to predict competitive outcomes, we ran the competition model 10,000 times, sampling the values of μ_{max} and K_S independently with replacement from the pool of available values. When assessing model performance for a particular subset, for example, for competitions at $T = 15$ ℃, μ_{max} and K_S were sampled independently from all values at $T = 15$ ℃ only. The analysis produced 10,000 values of proportion of competitive outcomes correctly predicted, for the 10,000 random parameter combinations. Figure S1 shows an example distribution, for the full dataset. The proportion of runs that correctly predicted a greater number of competitive outcomes than the model with the real values of μ_{max} and K_S is then given as the P value in Table 1. Therefore, P=0.05 means that 500 out of 10,000 random parameter combinations correctly predicted a greater proportion of competitive outcomes.

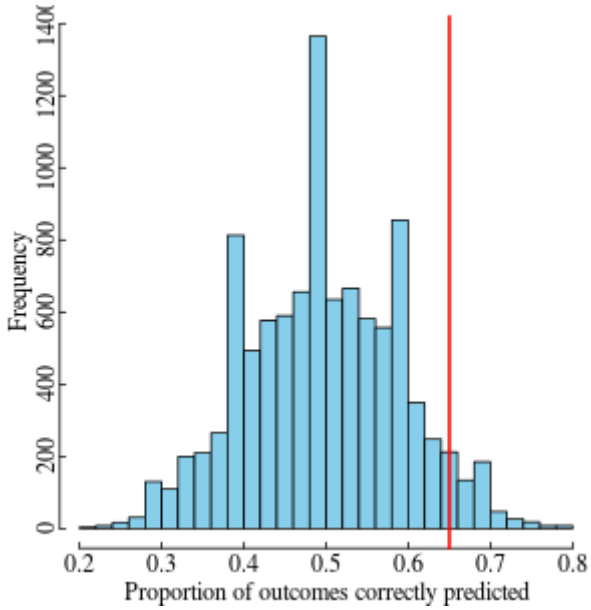

Figure S5A:

Histogram of the proportion of competitive outcomes correctly predicted for the 10,000 random combinations of μ_{max} and K_S. The red line indicates the performance of the model with the real values of μ_{max} and K_S. Here, there were 427 random parameter combinations that correctly predicted a greater number of competitive outcomes (P = 0.04 in Table 1).

S6. Simulations to compare the relative effects of mismatches

We use the competition model to assess the relative importance of mismatches in μ_{max} and K_S for determining the competitive outcome (Figure 3 in the main text). Mismatches are here defined as the ratios in the two traits between the two competitors. Ratios allow for direct comparison of the relative importance of mismatches in μ_{max} and K_S despite the different units. We assumed one competitor to have values of μ_{max} and K_S close to the respective median values across all species and treatments ($\mu_{max}=1$ and $K_S=0.15$ respectively), while the second competitor's μ_{max} and K_S values were chosen such that the ln ratio parameter space was evenly sampled. Results were insensitive to the choice of values for the fixed competitor. The reason to use ln ratios is to ensure that a ratio and its inverse are equidistant from a ratio of one. For all combinations of mismatches in traits we ran the competition model and extracted the proportion of total cells belonging to competitor A at day 14, for different starting nutrient concentrations (Figure 3a, b in the main text). As in the experiments, both species had a starting population density of 100 cells·mL^{-1}.

To compare the relative importance of mismatches in the two traits directly, we quantified by how much the competitive outcome changed due to a small increase in the ln ratio of μ_{max} and due to the same small increase in the ln ratio of K_S, and took their ratio. For example, a value of 10 means that a small increase in the mismatch in μ_{max} had a 10 times greater effect on the competitive outcome than did the same small increase in the mismatch in K_S (Figure 3c, d in the main text).

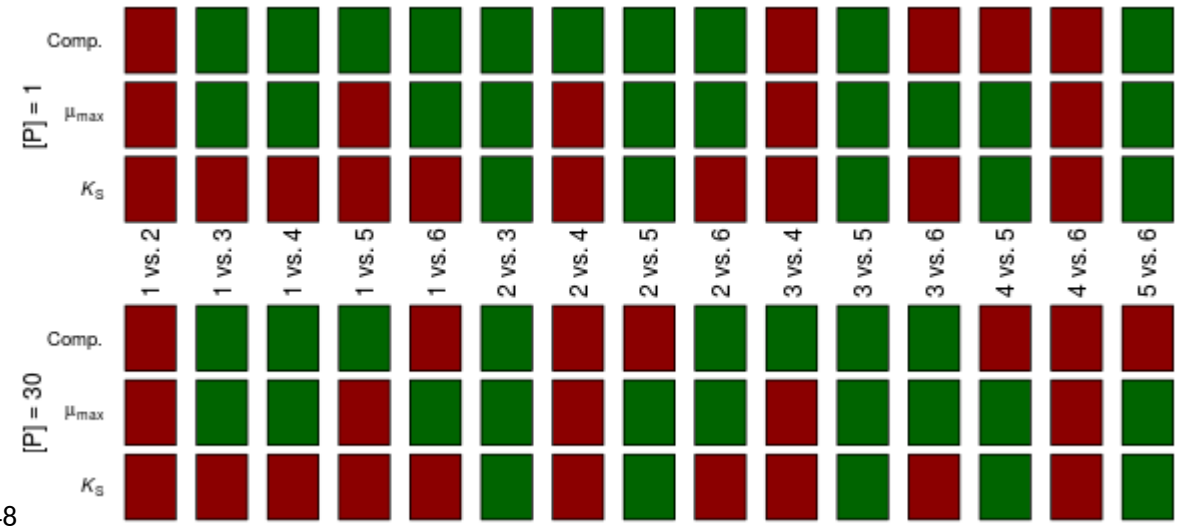

Figure S6A:
Reversals of competitive outcomes and traits due to temperature. Red boxes mean no reversal, while green boxes mean a reversal was observed between 15°C and 25°C. The different columns are for different competitions (e.g., species 1 vs. species 2). 'Comp.' refers to the experimentally observed competitive outcome (using the LDA discrimination method), while μ_{max} and K_S refer to species' traits that define the Monod curve (estimated using the mixed effects model). Results are shown for the two nutrient concentrations separately. For example, for species 1 vs. species 2, no reversals were observed in competitive outcomes or traits, while for species 1 vs. species 3, a reversal was observed in both the competitive outcome and μ_{max} (at both nutrient

858concentrations), but not in K_S . There were 18 reversals in competitive outcomes, of which 14
859coincided with reversals in mismatches in μ_{max} , and six with reversals in mismatches in K_S .
860Numbers represent the identity of the species: 1 = *Ankistrodesmus*, 2 = *Chlamydomonas*, 3 =
861*Chlorella*, 4 = *Monoraphidium*, 5 = *Scenedesmus* and 6 = *Selenastrum*.

862

S7: Robustness of the results to different statistical methods

Estimates for K_S and μ_{max} for the Monod model were obtained from a non-linear mixed model approach with the 'nlme' function in R, and were then used in models investigating competitive outcome throughout the manuscript. To test the robustness of the model to the method of determination of K_S and μ_{max}, we also fitted the Monod model to each species and temperature level using the 'nlsLM' function in the 'minpack.lm' package. Parameter estimation was achieved by running 1000 different random combination of starting parameters picked from a uniform distribution and returning the parameter set that returned the lowest AIC score. The two modelling approaches gave concordant results (Fig S7A). Thus in a second time, we used fits from this latter approach to feed in the later competition modelling (Table S7A). The results were extremely similar, with a slightly higher variance on the effect of K_S, which did not affect the predictive power of the model overall.

A second source of uncertainty was due to the method of discrimination between species. We used three different methods of discrimination, a linear discriminant analysis, a randomforest analysis and a recursive partitioning and regression tree (rpart, see Supplementary Material S2). Because the linear discriminant analysis was found to have the best predictive power overall (Table S2A), we used this method throughout the manuscript. However, we tested whether our results were robust to the method of species discrimination by comparing results from the competition model to predictions using the randomforest analysis and the rpart discrimination method, first with the mixed effect parameters from the Monod model (Table S7B and S7D), and second with the Monod parameters estimated using nonlinear least squares (Table S7C and S7E). The results were similar, with a lower predictive power of each variable and of the model due to the lower discrimination power of the two methods, but no significant discrepancies between species and temperature and nutrient conditions.

We also redid the figures comparing the relative effects of the mismatches (Fig S6A) with the Monod parameters estimated using nonlinear least squares or mixed effect model and the three discrimination analysis (LDA, rpart and randomforest, Figs S7B-S7F). The results were generally congruent.

894

895

Table S7A:

Same as Table 1 in the main text, using the LDA discrimination method for the competition data, and Monod parameters estimated using nonlinear least squares.

899

Subset	rP158	μ	μ_{max}	K_S	Model	N
Full dataset	0.70 (0.001)	0.62 (0.025)	0.60 (0.059)	0.37 (0.790)	0.65 (0.041)	60
By temperature						
$T = 15$ °C	0.80 (0.000)	0.67 (0.024)	0.57 (0.172)	0.43 (0.498)	0.67 (0.082)	30
$T = 25$ °C	0.60 (0.115)	0.57 (0.183)	0.63 (0.066)	0.30 (0.827)	0.63 (0.125)	30
By nutrient concentration						
$P = 1$ µmol·L^{-1}	0.70 (0.008)	0.57 (0.160)	0.60 (0.060)	0.40 (0.654)	0.67 (0.035)	30
$P = 30$ µmol·L^{-1}	0.70 (0.018)	0.67 (0.035)	0.60 (0.083)	0.33 (0.830)	0.63 (0.089)	30
By species						
Ankistrodesmus	0.90 (0.000)	0.45 (0.502)	0.85 (0.003)	0.35 (0.594)	0.80 (0.037)	20
Chlamydomonas	0.75 (0.004)	0.65 (0.050)	0.60 (0.112)	0.30 (0.768)	0.70 (0.047)	20
Chlorella	0.70 (0.056)	0.85 (0.004)	0.70 (0.087)	0.30 (0.695)	0.75 (0.085)	20
Monoraphidium	0.60 (0.084)	0.65 (0.026)	0.50 (0.237)	0.50 (0.239)	0.65 (0.064)	20
Scenedesmus	0.80 (0.000)	0.70 (0.004)	0.60 (0.062)	0.30 (0.833)	0.60 (0.128)	20
Selenastrum	0.45 (0.512)	0.40 (0.699)	0.35 (0.737)	0.45 (0.389)	0.40 (0.757)	20

900

901

Table S7B:

Same as Table 1 in the main text, using the rpart discrimination method for the competition data, and Monod parameters estimated using the mixed effects model.

905

Subset	rP158	μ	μ_{max}	K_S	Model	N
Full dataset	0.65 (0.010)	0.63 (0.015)	0.52 (0.216)	0.47 (0.405)	0.62 (0.065)	60
By temperature						
$T = 15$ °C	0.77 (0.000)	0.63 (0.051)	0.53 (0.255)	0.47 (0.413)	0.63 (0.139)	30
$T = 25$ °C	0.53 (0.240)	0.63 (0.058)	0.50 (0.305)	0.47 (0.399)	0.60 (0.145)	30
By nutrient concentration						
$P = 1$ µmol·L^{-1}	0.63 (0.049)	0.63 (0.047)	0.47 (0.360)	0.53 (0.172)	0.63 (0.065)	30
$P = 30$ µmol·L^{-1}	0.67 (0.032)	0.63 (0.069)	0.57 (0.138)	0.40 (0.638)	0.60 (0.145)	30
By species						
Ankistrodesmus	0.85 (0.000)	0.50 (0.366)	0.80 (0.006)	0.40 (0.523)	0.75 (0.049)	20
Chlamydomonas	0.70 (0.023)	0.70 (0.024)	0.55 (0.195)	0.35 (0.649)	0.65 (0.092)	20
Chlorella	0.70 (0.045)	0.85 (0.001)	0.60 (0.197)	0.35 (0.589)	0.70 (0.100)	20
Monoraphidium	0.55 (0.179)	0.60 (0.082)	0.45 (0.385)	0.65 (0.019)	0.60 (0.123)	20

Scenedesmus	0.75 (0.003)	0.75 (0.004)	0.45 (0.411)	0.55 (0.182)	0.55 (0.291)	20
Selenastrum	0.35 (0.770)	0.40 (0.609)	0.25 (0.855)	0.50 (0.262)	0.45 (0.487)	20

906

Table S7C :

Same as Table 1 in the main text, using the rpart discrimination method for the competition data, and Monod parameters estimated using nonlinear least squares.

Subset	rP158	μ	μ_{max}	K_S	Model	N
Full dataset						
	0.65 (0.009)	0.63 (0.015)	0.52 (0.221)	0.43 (0.532)	0.62 (0.071)	60
By temperature						
$T = 15$ °C	0.77 (0.001)	0.63 (0.045)	0.53 (0.254)	0.47 (0.411)	0.63 (0.134)	30
$T = 25$ °C	0.53 (0.245)	0.63 (0.058)	0.50 (0.307)	0.40 (0.581)	0.60 (0.161)	30
By nutrient concentration						
$P = 1$ µmol·L^{-1}	0.63 (0.043)	0.63 (0.044)	0.47 (0.367)	0.50 (0.250)	0.63 (0.065)	30
$P = 30$ µmol·L^{-1}	0.67 (0.036)	0.63 (0.068)	0.57 (0.139)	0.37 (0.740)	0.60 (0.143)	30
By species						
Ankistrodesmus	0.85 (0.000)	0.50 (0.367)	0.80 (0.005)	0.40 (0.526)	0.75 (0.047)	20
Chlamydomonas	0.70 (0.023)	0.70 (0.025)	0.55 (0.198)	0.35 (0.657)	0.65 (0.093)	20
Chlorella	0.70 (0.042)	0.85 (0.001)	0.60 (0.192)	0.35 (0.585)	0.70 (0.103)	20
Monoraphidium	0.55 (0.182)	0.60 (0.082)	0.45 (0.389)	0.55 (0.111)	0.60 (0.122)	20
Scenedesmus	0.75 (0.004)	0.75 (0.004)	0.45 (0.412)	0.45 (0.413)	0.55 (0.296)	20
Selenastrum	0.35 (0.771)	0.40 (0.608)	0.25 (0.855)	0.50 (0.263)	0.45 (0.484)	20

Table S7D:

Same as Table 1 in the main text, using the random forests discrimination method for the competition data, and Monod parameters estimated using the mixed effects model.

Subset	rP158	μ	μ_{max}	K_S	Model	N
Full dataset						
	0.70 (0.001)	0.62 (0.032)	0.57 (0.118)	0.43 (0.559)	0.68 (0.021)	60
By temperature						
$T = 15$ °C	0.80 (0.000)	0.67 (0.023)	0.57 (0.172)	0.43 (0.489)	0.67 (0.084)	30
$T = 25$ °C	0.60 (0.130)	0.57 (0.199)	0.57 (0.196)	0.43 (0.502)	0.70 (0.058)	30
By nutrient concentration						
$P = 1$ µmol·L^{-1}	0.67 (0.039)	0.60 (0.119)	0.50 (0.312)	0.53 (0.221)	0.70 (0.027)	30
$P = 30$ µmol·L^{-1}	0.73 (0.003)	0.63 (0.058)	0.63 (0.032)	0.33 (0.844)	0.67 (0.038)	30
By species						
Ankistrodesmus	0.90 (0.000)	0.45 (0.512)	0.85 (0.005)	0.35 (0.602)	0.80 (0.041)	20
Chlamydomonas	0.80 (0.000)	0.60 (0.100)	0.65 (0.035)	0.25 (0.891)	0.75 (0.011)	20
Chlorella	0.70 (0.066)	0.85 (0.005)	0.60 (0.203)	0.40 (0.516)	0.75 (0.087)	20
Monoraphidium	0.60 (0.088)	0.65 (0.028)	0.50 (0.231)	0.60 (0.062)	0.65 (0.062)	20
Scenedesmus	0.80 (0.001)	0.80 (0.001)	0.50 (0.297)	0.50 (0.291)	0.60 (0.190)	20

Selenastrum	0.40 (0.696)	0.35 (0.843)	0.30 (0.817)	0.50 (0.261)	0.55 (0.280)	20

Table S7E:

Same as Table 1 in the main text, using the random forests discrimination method for the competition data, and Monod parameters estimated using nonlinear least squares.

Subset	**rP158**	μ	μ_{max}	K_S	**Model**	**N**
Full dataset	0.70 (0.002)	0.62 (0.034)	0.57 (0.122)	0.40 (0.674)	0.68 (0.020)	60
By temperature						
$T = 15$ °C	0.80 (0.000)	0.67 (0.025)	0.57 (0.179)	0.43 (0.483)	0.67 (0.087)	30
$T = 25$ °C	0.60 (0.128)	0.57 (0.193)	0.57 (0.202)	0.37 (0.659)	0.70 (0.063)	30
By nutrient concentration						
$P = 1$ µmol·L^{-1}	0.67 (0.038)	0.60 (0.118)	0.50 (0.314)	0.50 (0.319)	0.70 (0.028)	30
$P = 30$ µmol·L^{-1}	0.73 (0.004)	0.63 (0.057)	0.63 (0.035)	0.30 (0.908)	0.67 (0.040)	30
By species						
Ankistrodesmus	0.90 (0.000)	0.45 (0.502)	0.85 (0.003)	0.35 (0.603)	0.80 (0.037)	20
Chlamydomonas	0.80 (0.000)	0.60 (0.094)	0.65 (0.040)	0.25 (0.889)	0.75 (0.010)	20
Chlorella	0.70 (0.062)	0.85 (0.002)	0.60 (0.196)	0.40 (0.523)	0.75 (0.085)	20
Monoraphidium	0.60 (0.076)	0.65 (0.027)	0.50 (0.237)	0.50 (0.242)	0.65 (0.062)	20
Scenedesmus	0.80 (0.001)	0.80 (0.000)	0.50 (0.295)	0.40 (0.535)	0.60 (0.195)	20
Selenastrum	0.40 (0.701)	0.35 (0.840)	0.30 (0.817)	0.50 (0.266)	0.55 (0.279)	20

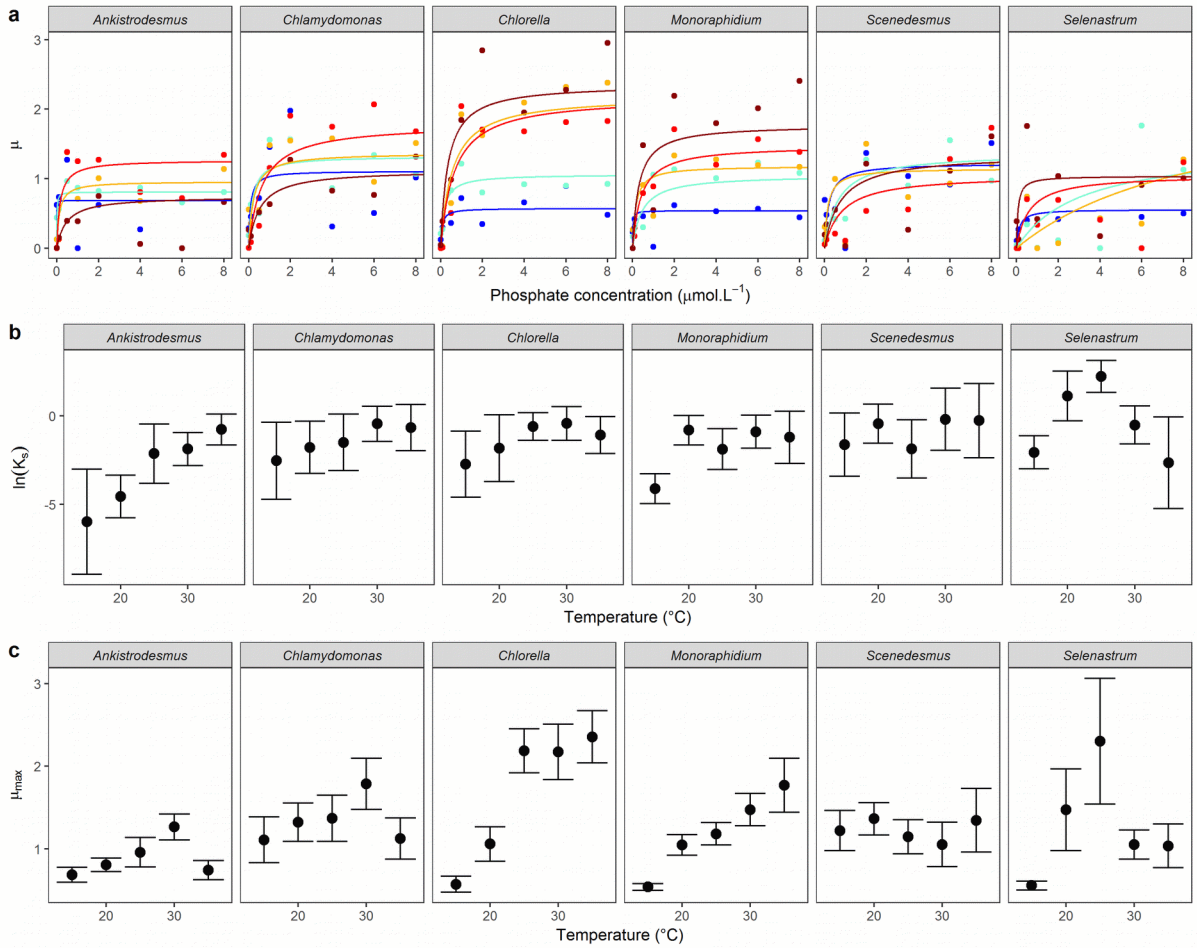

926

927**Fig S7A:**

928 **(a)** Mean Monod curves for each species growth rate estimated using nonlinear least squares. 929Growth rate μ as a function of phosphate concentration in the medium (µmol·L^{-1}) and 930temperature (from blue: 15°C to dark red: 35°C). Points represent the mean of the 3 931replicates. Note that the phosphate concentration levels in the experiment go from 0.01 to 50 932µmol·L^{-1} but the x-axis was cut at 8 µmol·L^{-1} for clarity. **(b)** Half-saturation coefficient K_S 933(mean ± 95%CI) **(c)** Maximum growth rate μ_{max} (mean ± 95%CI).

934

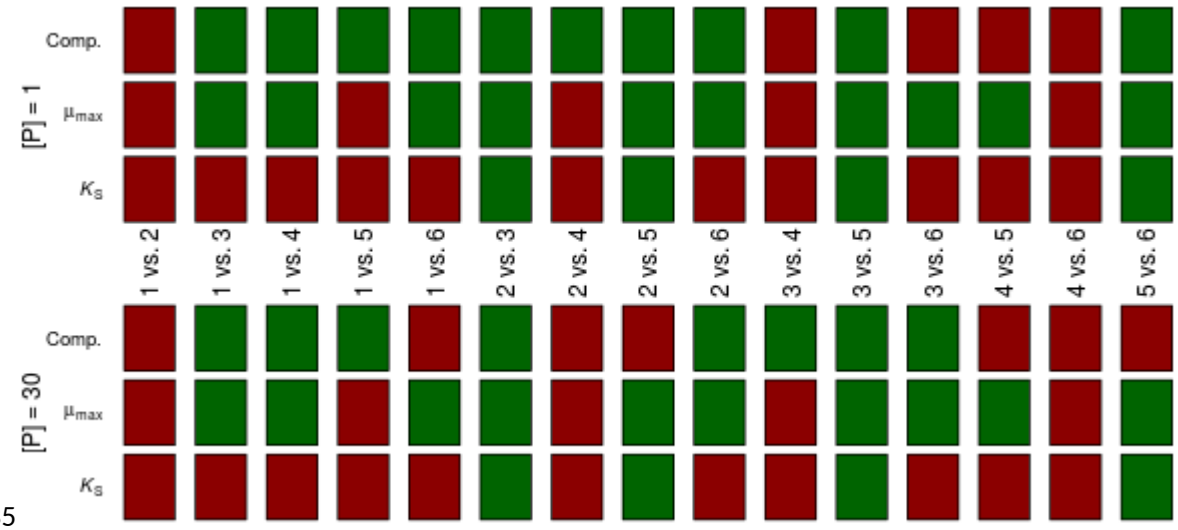

Figure S7B: Same as Figure SX, using the LDA discrimination method in the competition data, and nonlinear least squares parameter estimates of the Monod model for the traits. There were 18 reversals in competitive outcomes, of which 14 coincided with reversals in mismatches in μ_{max}, and six with reversals in mismatches in K_S.

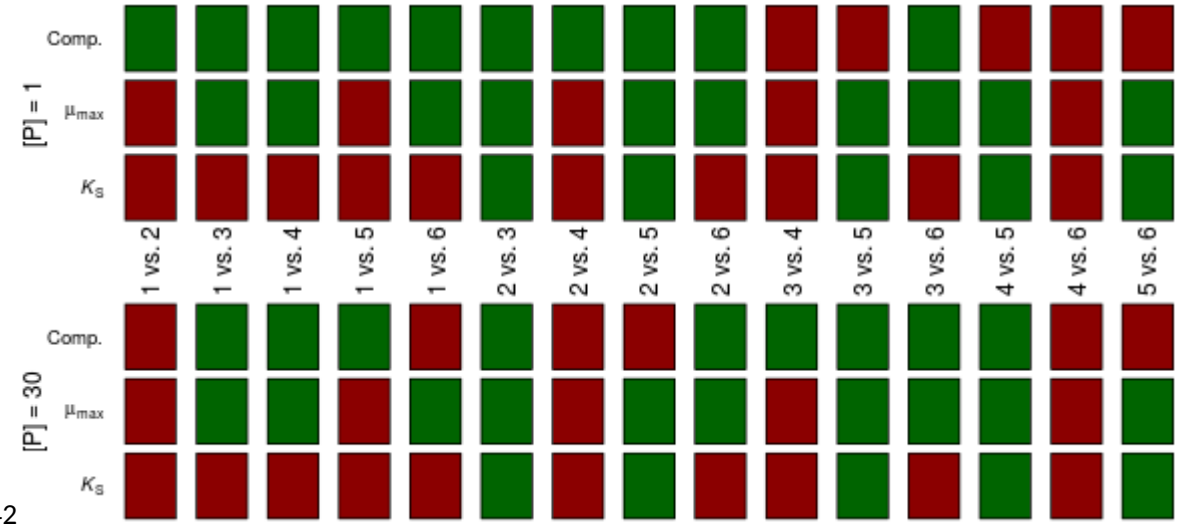

Figure S7C: Same as Figure SX, using the rpart discrimination method in the competition data, and parameter estimates from the mixed effects model of the Monod model for the traits. There were 19 reversals in competitive outcomes, of which 14 coincided with reversals in mismatches in μ_{max}, and five with reversals in mismatches in K_S.

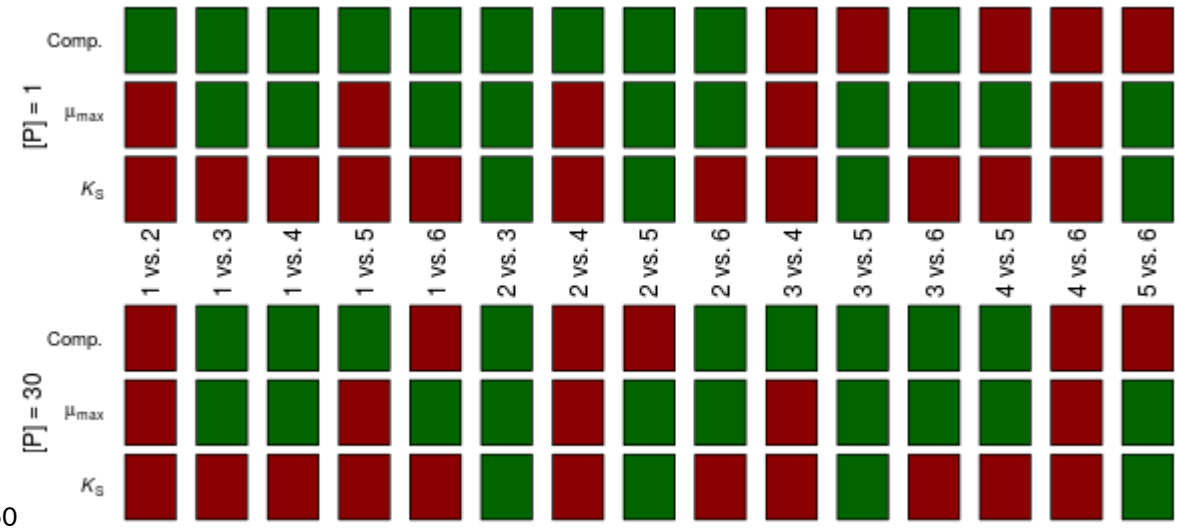

Figure S7D: Same as Figure SX, using the rpart discrimination method in the competition data, and parameter estimates from nonlinear least squares fit of the Monod model for the traits. There were 19 reversals in competitive outcomes, of which 14 coincided with reversals in mismatches in μ_{max}, and four with reversals in mismatches in K_S.

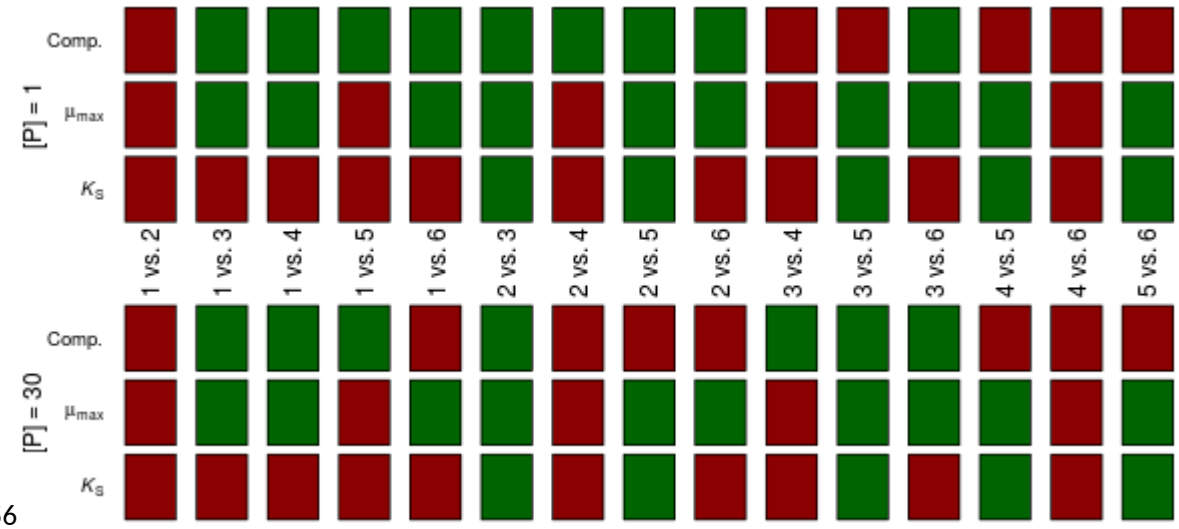

Figure S7E: Same as Figure SX, using the random forests discrimination method in the competition data, and parameter estimates from the mixed effects model of the Monod model for the traits. There were 16 reversals in competitive outcomes, of which 12 coincided with reversals in mismatches in μ_{max}, and four with reversals in mismatches in K_S.

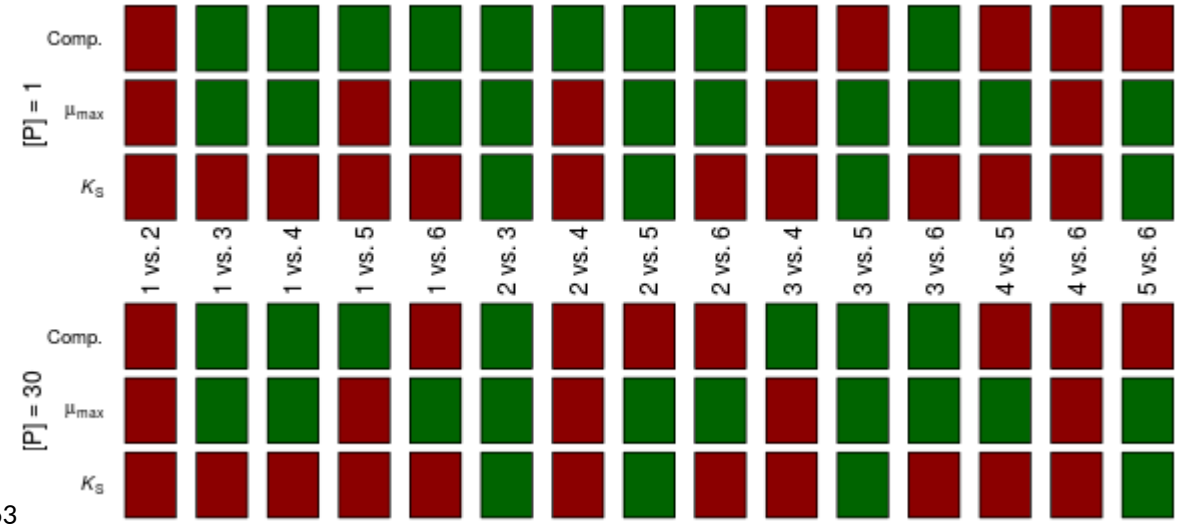

963

964Figure S7F: Same as Figure SX, using the random forests discrimination method in the
965competition data, and parameter estimates from nonlinear least squares fit of the Monod
966model for the traits. There were 16 reversals in competitive outcomes, of which 12 coincided
967with reversals in mismatches in μ_{max} , and four with reversals in mismatches in K_S .

968

969